

# Fucosylated Chondroitin Sulfate 9–18 Oligomers Exhibit Molecular Size-Independent Antithrombotic Activity while Circulating in the Blood

Lufeng Yan, Danli Wang, Yanlei Yu, Fuming Zhang, Xingqian Ye, Robert J. Linhardt,\* and Shiguo Chen\*



Cite This: *ACS Chem. Biol.* 2020, 15, 2232–2246



Read Online

ACCESS |



Metrics & More

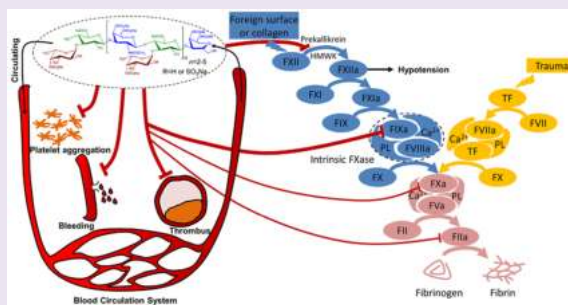


Article Recommendations



Supporting Information

**ABSTRACT:** Fucosylated chondroitin sulfate (FCS) oligosaccharides extracted from sea cucumber and depolymerized exhibit potent anticoagulant activity. Knowledge of the antithrombotic activity of different size oligosaccharides and their fucose (Fuc) branch sulfation pattern should promote their development for clinical applications. We prepared highly purified FCS trisaccharide repeating units from hexasaccharide (6-mer) to octadecasaccharide (18-mer), including those with 2,4-disulfated and 3,4-disulfated Fuc branches. All 10 oligosaccharides were identified by their nuclear magnetic resonance structures and ESI-FTMS spectroscopy. *In vitro* anticoagulant activities and surface plasmon resonance binding tests indicated those of larger molecular sizes and 2,4-disulfated Fuc branches showed stronger anticoagulant effects with respect to anti-FXase activity, as well as stronger binding to FIXa among various clotting proteins. However, both types of FCS 9-mer to 18-mer exhibited molecular size-independent potent antithrombotic activity *in vivo* at the same dose. In addition, both types of the FCS 6-mer exhibited favorable antithrombotic activity *in vivo*, although they showed weak anticoagulant activity *in vitro*. Combining absorption and metabolism studies, we conclude that FCS 9–18 oligomers could remain in the circulation to interact with various clotting proteins to prevent thrombus formation, and appreciable quantities of these oligomers could be excreted through the kidneys. All FCS 9–18 oligomers also resulted in no bleeding, hypotension, or platelet aggregation risk during blood circulation. Thus, FCS 9–18 oligomers with 2,4-disulfated or 3,4-disulfated Fuc branches exhibit potent and safe antithrombotic activity needed for clinical applications.



With the general improvement of human living standards and the aging of the population, thrombotic disease has become a serious human health concern over the past few decades. Heparin and low-molecular weight heparins (LMWHs) are in widespread use as anticoagulants for the treatment of thrombotic diseases, especially during surgical situations.<sup>1–4</sup> However, heparin and LMWHs always have the risk of serious bleeding during therapy and cannot be orally administered.<sup>5–7</sup> Thus, researchers have continued to search for other effective and safer anticoagulant drugs.

Fucosylated chondroitin sulfate (FCS), isolated from sea cucumber, has outstanding *in vitro* anticoagulant and antithrombotic activities and might also achieve *in vivo* anticoagulant and antithrombotic effects on oral administration after appropriate modification.<sup>8–11</sup> FCS oligosaccharides of a particular molecular size range can show potent *in vivo* anticoagulant and antithrombotic activities by selective inhibition of the intrinsic factor Xase (FXase), avoiding side effects such as factor XII (FXII) activation, platelet aggregation, and increased bleeding risk.<sup>12–15</sup>

While the chemical synthesis of FCS oligosaccharides has been possible,<sup>16–18</sup> it is much easier and more cost-effective to prepare FCS oligosaccharides derived from polysaccharides. The structural differences of FCS polysaccharides from various sea cucumbers mainly result from differences in the sulfation pattern of Fuc branches.<sup>19,20</sup> Obtaining effective FCS oligosaccharides with a different sulfation pattern of Fuc branches could expand the clinical application of these new anticoagulant agents.

Many chemical or physical methods have been reported for preparing FCS oligosaccharides, such as acid-catalyzed hydrolysis,<sup>60</sup> Co irradiation, and free-radical depolymeriza-

Received: May 29, 2020

Accepted: July 28, 2020

Published: July 28, 2020



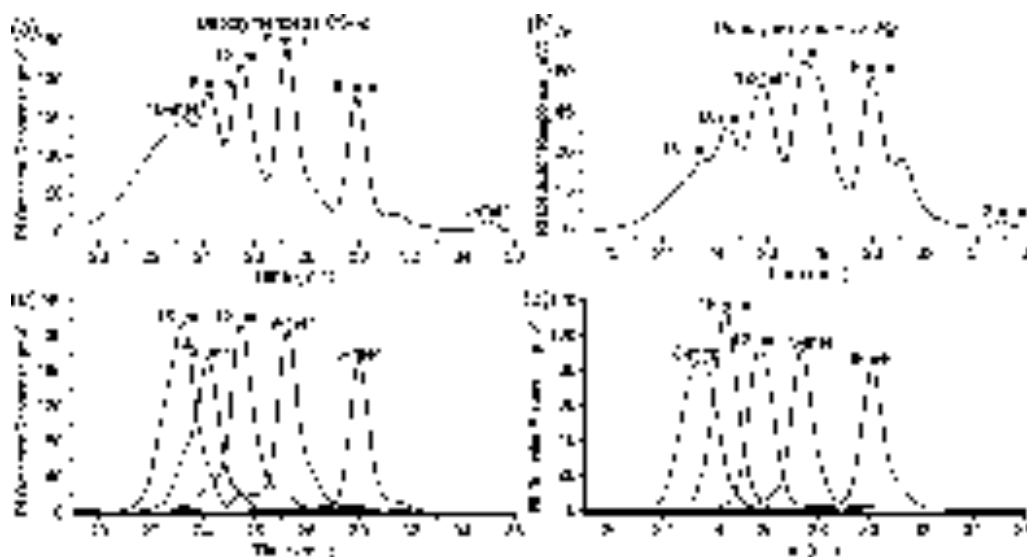


**Figure 1.** HPGPC profiles of (a) depolymerized FCS-*Ib*, (b) depolymerized FCS-*Pg*, (c) separated FCS-*Ib* oligomers, and (d) separated FCS-*Pg* oligomers, analyzed using a Superdex Peptide 10/300 GL column (10 mm × 300 mm) by a refractive index detector. Samples were size-fractionated using 0.2 M NaCl as the eluent at a flow rate of 0.4 mL/min.

tion.<sup>21–24</sup> However, these methods will all require high-purity FCS polysaccharide as a starting material to avoid fragments of a second sea cucumber polysaccharide, fucoidan. FCS oligosaccharide preparation methods generally rely on anion-exchange chromatography for polysaccharide purification and gel permeation chromatography for oligosaccharide fractionation, but both methods are labor-intensive and costly and, thus, are inappropriate for large-scale preparation.

We recently established a method for the rapid preparation of purified FCS oligosaccharides from dry sea cucumber, *Pearsonothuria graeffei*. The resulting FCS oligosaccharides showed potent anticoagulant and antithrombotic activities by selectively inhibiting the intrinsic coagulation pathway while avoiding side effects such as bleeding and hypotension.<sup>25</sup> The chemical process, N-deacetylation–deaminative cleavage, used by this method is the same as that currently relied on in the preparation of LMWHs from heparin.<sup>26,27</sup> The molecular size of the resulting FCS oligosaccharides prepared by this method was optimized for 6–18 oligomers, resulting in easy production quality control. Prior to the clinical application of FCS 6–18 oligomers, the effects of the molecular size and sulfation pattern of the Fuc branches on anticoagulant and antithrombotic activity and side effects need to be resolved. In addition, because there are no mammalian enzymes that can degrade FCS oligomers because of their Fuc branches,<sup>28</sup> the clearance of FCS oligomers after subcutaneous injection needs to be explored.

On the basis of previous publications,<sup>14,25</sup> the study presented here investigated and compared the anticoagulant and antithrombotic activity and potential side effects of 10 FCS oligomers obtained from two different varieties of sea cucumbers. The FCS-*Ib* oligomers were prepared from sea cucumber *Isoetichopus badionotus* (*Ib*), and the FCS-*Pg* oligomers were prepared from sea cucumber *P. graeffei* (*Pg*). Fluorescence labeling was used to study the absorption and metabolism of FCS oligomers after subcutaneous administration. These studies should serve as reference for the large-

scale production of FCS oligomers and their clinical applications.

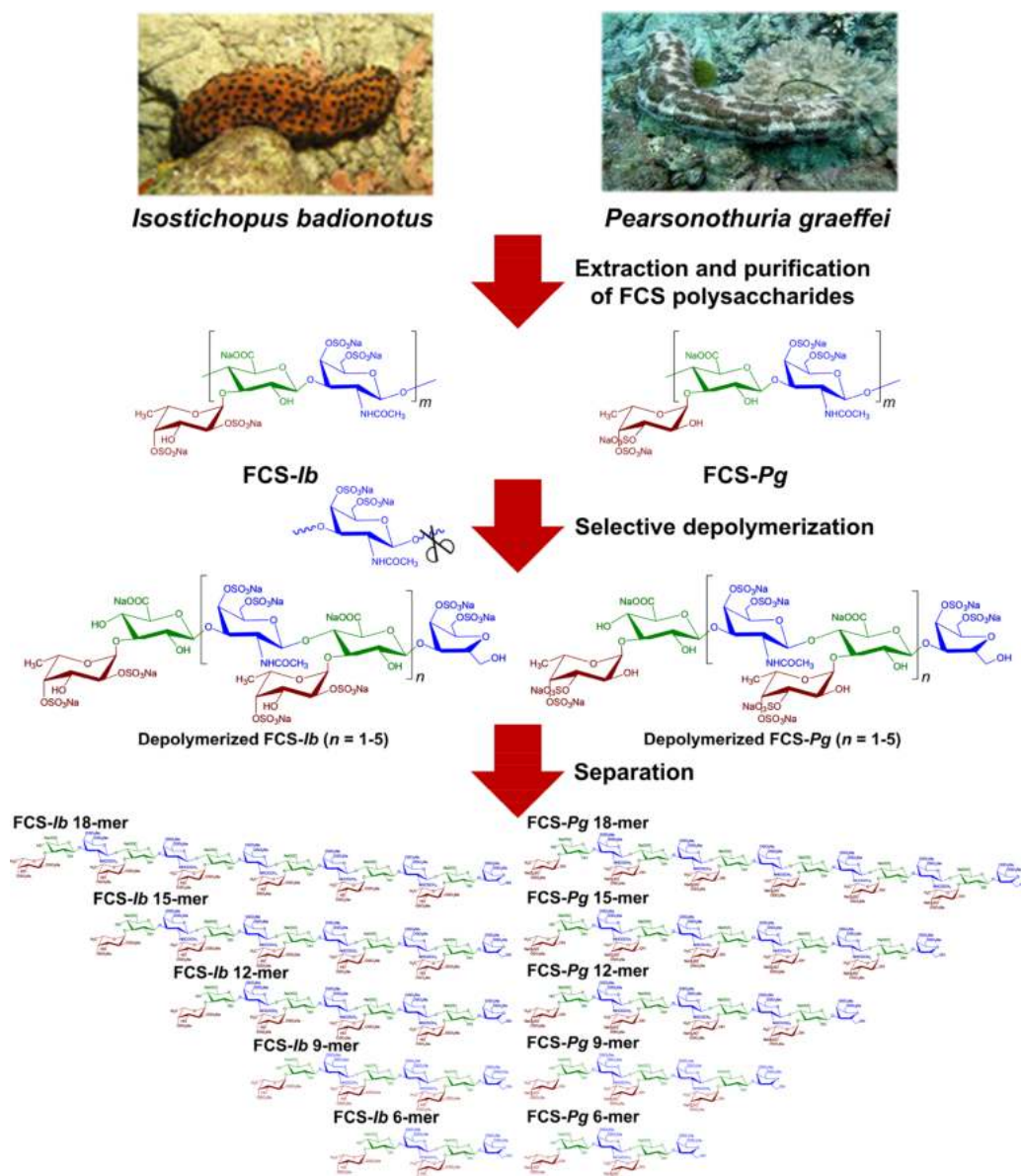
## RESULTS AND DISCUSSION

**Efficient Separation of FCS Oligomers.** Native FCS polysaccharides, FCS-*Ib* and FCS-*Pg*, were isolated and purified from *Ib* and *Pg*, respectively. Their structures, including mainly trisaccharide repeating units and unique sulfation on Fuc branches, were previously established.<sup>10,29</sup> We next used a partial N-deacetylation–deaminative cleavage method to selectively depolymerize the glycosidic bond of D-GalNAc4S6S- $\beta$ 1,4-D-GlcA on the native FCS polysaccharides with no obvious sulfation or Fuc branch loss.<sup>14,30,31</sup>

The HPGPC profiles of partially depolymerized FCS-*Ib* and partially depolymerized FCS-*Pg* are shown in panels a and b of Figure 1, respectively. This treatment afforded a mixture of homogeneous oligosaccharides with trisaccharide repeating units, which were identified as the 3-mer, 6-mer, 9-mer, 12-mer, 15-mer, and 18-mer.<sup>13</sup> However, chromatographic peaks in depolymerized FCS-*Pg*, especially the 6-mer and 9-mer, were broad and showed some peak splitting, suggesting the partial vacancy of the Fuc branch from original polysaccharides as observed in our previous study.<sup>29</sup> Thus, efficient gel permeation chromatography column (1.0 cm × 120 cm) packed with Superdex 30 prep grade gel filtration resin was used to separate the mixture of depolymerized FCS. Combined with analysis using a Superdex Peptide 10/300 GL column, highly purified FCS oligomers, ranging from the 6-mer to 18-mer, were obtained from both sea cucumbers (panels c and d of Figure 1, respectively). The entire preparation process for FCS oligomers is summarized in Scheme 1.

**Structural Characterization of FCS Oligomers.** We characterized the structure of these highly purified FCS oligomers based on the published native FCS structure.<sup>8,10</sup> In the nuclear magnetic resonance (NMR) spectra of the FCS-*Ib* 6-mer (Figure 2a,c), the H-1 proton of each residue could be assigned to the peaks at 5.68, 5.56, 4.52, 4.53, 4.57, and

Scheme 1. Preparation of Highly Purified FCS 6–18 Oligomers with Potential Structures



3.69/3.81 ppm for middle Fuc, terminal Fuc, nonreducing terminal GlcA, reducing terminal GlcA, GalNAc, and 2,5-anhydro-D-talitol (anTal-ol), respectively. The C-1 signals at 97.2, 97.3, 104.2, 102.4, 100.6, and 61.4 ppm, respectively, were also similarly assigned. Compared with the unsulfated monosaccharide,<sup>10</sup> the downfield shift of protons caused by sulfation indicated that Fuc is sulfated at the C-2 and C-4 positions, and GalNAc and anTal-ol are both sulfated at the C-4 and C-6 positions. In addition, ESI-FTMS analysis of the FCS-Ib 6-mer revealed an ion at  $m/z$  411.74 for  $[M - 4H]^{4-}$  and  $m/z$  549.32 for  $[M - 3H]^{3-}$ , confirming a molecular formula of  $C_{38}H_{61}O_{54}N_1S_8$  (Figure 2e). On the basis of these data, the structure of the FCS-Ib 6-mer was determined to be L-Fuc2,4diS- $\alpha$ 1,3-D-GlcA- $\beta$ 1,3-D-GalNAc4,6diS- $\beta$ 1,4-[L-Fuc2,4diS- $\alpha$ 1,3]-D-GlcA- $\beta$ 1,3-D-anTal-ol4,6diS as the majority.

The NMR spectra of the FCS-Pg 6-mer were similar to those of the FCS-Ib 6-mer (Figure 2b,d). The major distinction was that the Fuc of the FCS-Pg 6-mer was sulfated at positions C-3 and C-4, based on the downfield shifts of H-3 and H-4 signals. The ESI-FTMS analysis of the FCS-Pg 6-mer revealed an ion at  $m/z$  411.74 for  $[M - 4H]^{4-}$  and  $m/z$  549.32 for  $[M - 3H]^{3-}$ , confirming a molecular formula of  $C_{38}H_{61}O_{54}N_1S_8$  (Figure 2f). Thus, the structure of the FCS-Pg 6-mer was mainly established as L-Fuc3,4diS- $\alpha$ 1,3-D-GlcA- $\beta$ 1,3-D-GalNAc4,6diS- $\beta$ 1,4-[L-Fuc3,4diS- $\alpha$ 1,3]-D-GlcA- $\beta$ 1,3-D-anTal-ol4,6diS. Using the same method, we confirmed the structure of FCS-Ib 9–18 oligomers mainly as L-Fuc2,4diS- $\alpha$ 1,3-D-GlcA- $\beta$ 1,3]-{D-GalNAc4,6diS- $\beta$ 1,4-[L-Fuc2,4diS- $\alpha$ 1,3]-D-GlcA- $\beta$ 1,3}- $_n$ -D-anTal-ol4,6diS ( $n = 2-5$ ) (Figures S1–S4 and S9) and the structure of FCS-Pg 9–18 oligomers mainly as L-Fuc3,4diS-



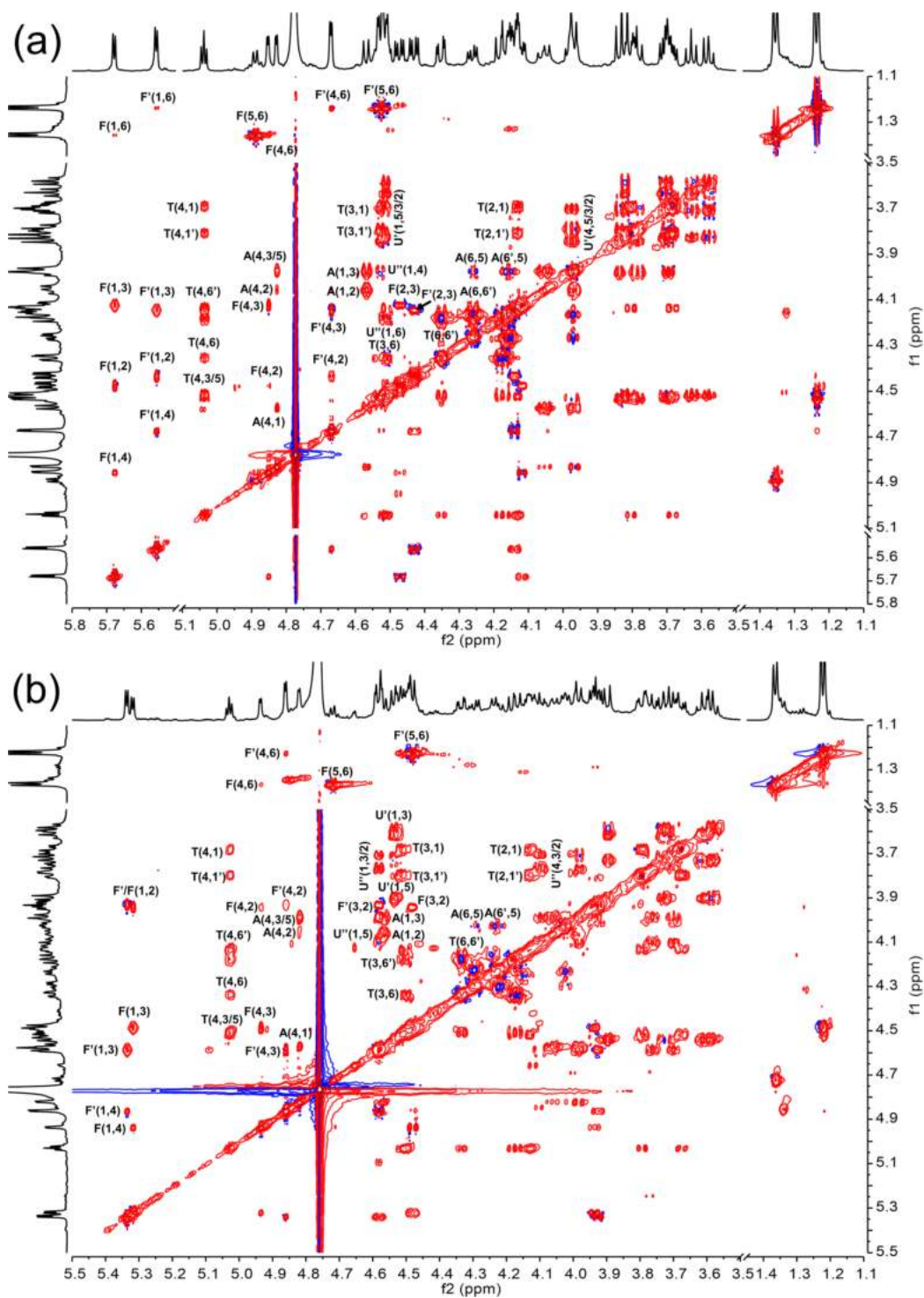


Figure 2. continued

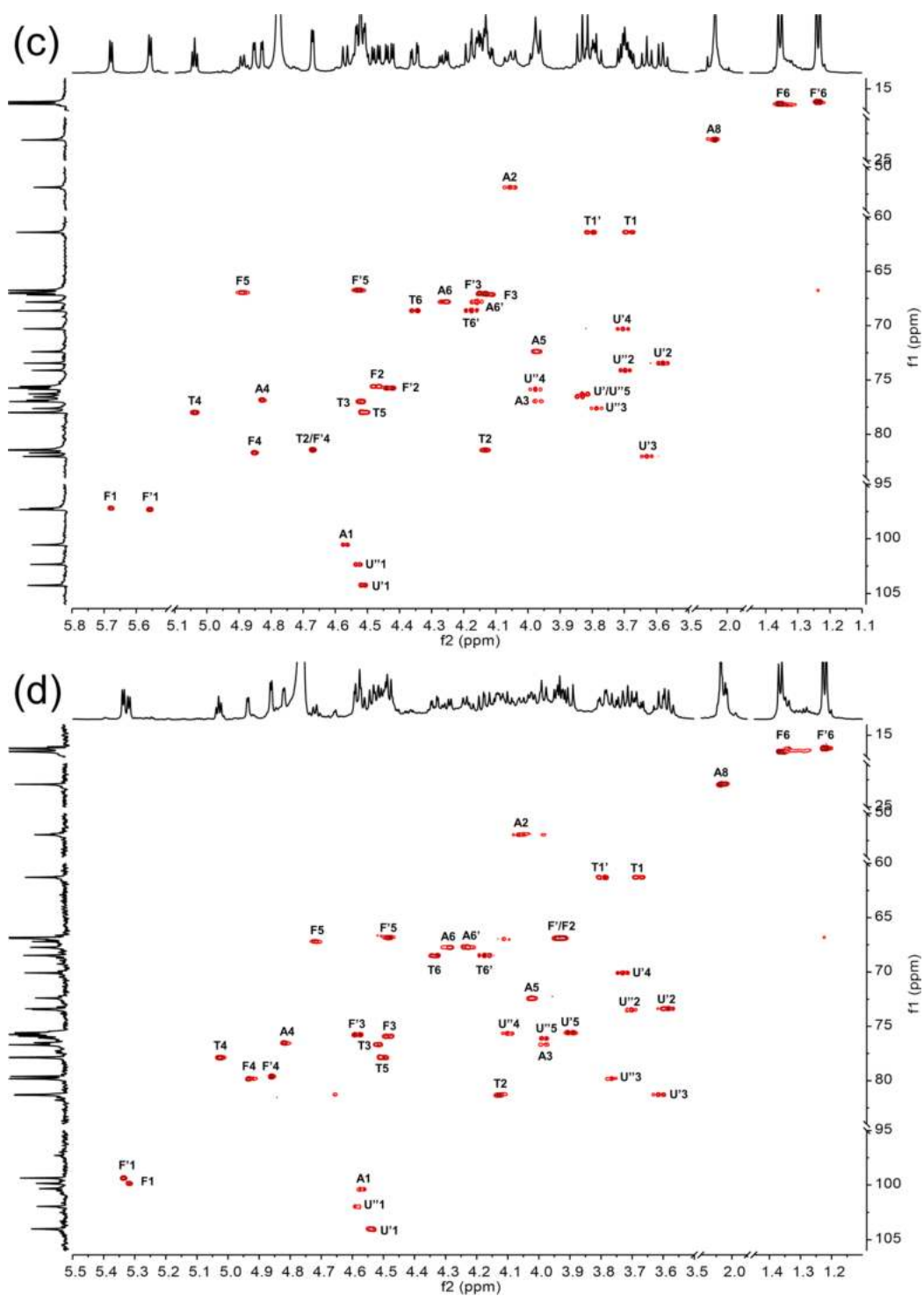
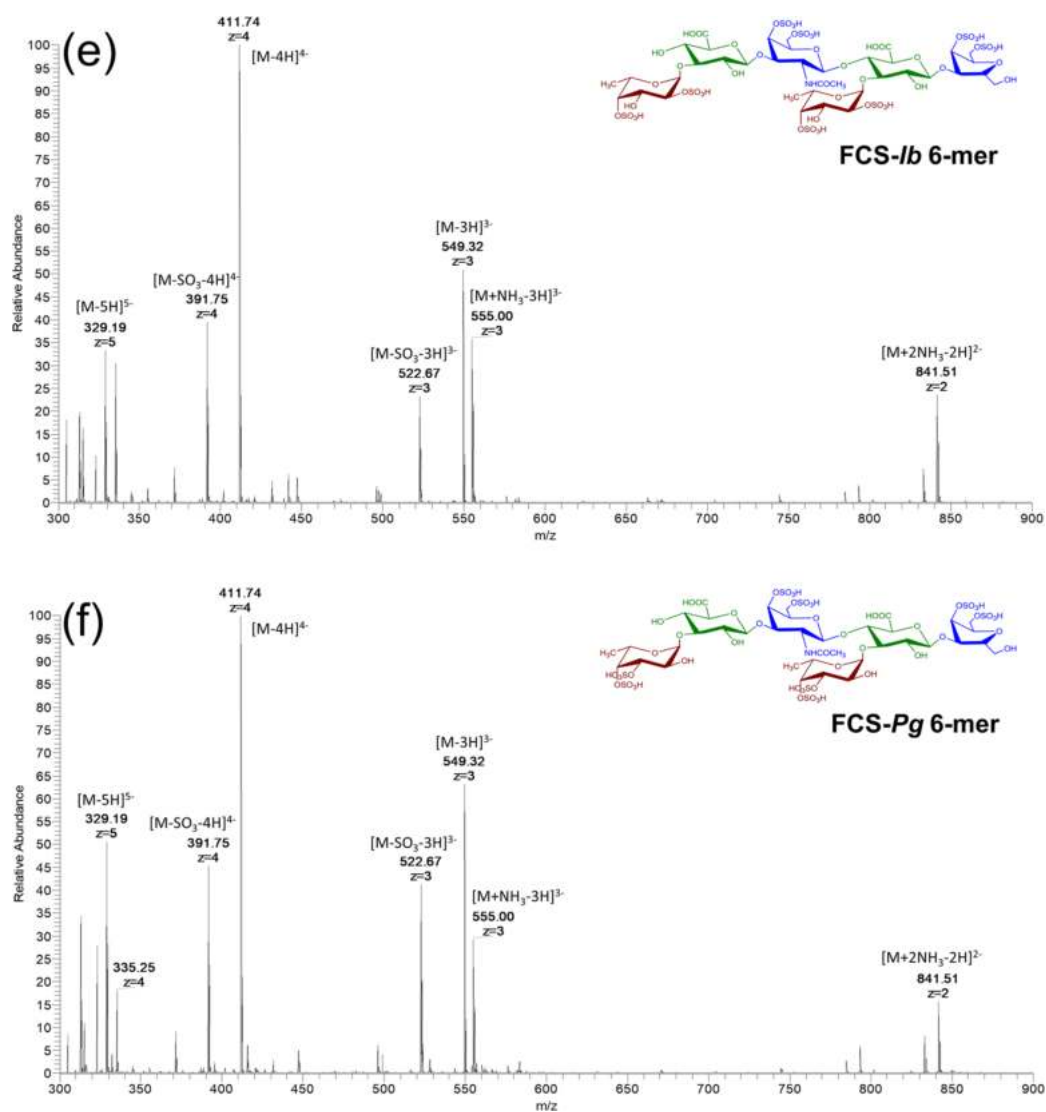


Figure 2. continued



**Figure 2.** (a)  $^1\text{H}$ – $^1\text{H}$  TOCSY spectrum and (c)  $^1\text{H}$ – $^{13}\text{C}$  HSQC spectrum of the FCS-*Ib* 6-mer. (b)  $^1\text{H}$ – $^1\text{H}$  TOCSY spectrum and (d)  $^1\text{H}$ – $^{13}\text{C}$  HSQC spectrum of the FCS-*Pg* 6-mer. Labels are the same as those described in Tables S1 and S2. ESI-FTMS spectrograms of (e) the FCS-*Ib* 6-mer and (f) the FCS-*Pg* 6-mer with matched structures. The patterns of sulfation in the Fuc residues are based on NMR spectral analysis.

$\alpha 1,3\text{-D-GlcA-}\beta 1,3\text{-}\{D\text{-GalNAc}4,6\text{diS-}\beta 1,4\text{-}[L\text{-Fuc}3,4\text{diS-}\alpha 1,3\text{-}]D\text{-GlcA-}\beta 1,3\text{-}\}_n\text{-D-anTal-ol}4,6\text{diS}$  ( $n = 2\text{--}5$ ) (Figures S5–S8 and S10). All of the  $^1\text{H}$  and  $^{13}\text{C}$  chemical shifts of FCS oligomers are listed in Tables S1 and S2, although it looks like there is some contamination from high- and low-molecular weight oligomers in fractions like the FCS-*Ib* 9-mer, FCS-*Ib* 12-mer, and FCS-*Ib* 15-mer as reflected by uneven HPGPC curves (Figure 1c). From the NMR and MS spectra, it could be confirmed that all of these oligomer fractions are of high purity with little surrounding contamination and responsible for further structure–activity study.

**FCS Oligomers Exhibit Effective Anticoagulant Activities by Selectively Inhibiting FXase.** The anticoagulant activities of FCS oligomers were evaluated using the activated partial thromboplastin time (APTT) and thrombin time (TT) of plasma clotting assays (Table 1) to determine their ability to inhibit blood clotting through the intrinsic or

common pathways of the coagulation cascade. Both FCS-*Ib* oligomers and FCS-*Pg* oligomers showed intrinsic anticoagulant activity as only prolonging APTT. Their molecular size had a significant impact on this activity for both types of FCS oligomers. The concentration of the FCS 18-mer required to double the APTT was similar to that of LMWHs. With the decrease in molecular size, the concentration required to double the APTT was increased. The concentration of the FCS 9-mer required to double the APTT was  $\sim 3$ -fold higher than that of the FCS 18-mer. The FCS 6-mer showed weak intrinsic anticoagulant activity as reflected by APTT. For the same oligomer size, the FCS-*Ib* oligomer showed intrinsic anticoagulant activity slightly higher than that of the FCS-*Pg* oligomer as reflected by APTT. This result was consistent with the previous study that showed that native FCS-*Ib* showed stronger intrinsic anticoagulant activity than native FCS-*Pg*.<sup>8,10</sup>

Table 1. Anticoagulant Properties of FCS Oligomers and Their Effects on Coagulation Factors with a Cofactor

compd	APTT <sup>a</sup>		TT <sup>a</sup>		anti-FIIa/AT		anti-FXa/AT		anti-FXase	
	$\mu\text{g/mL}^b$	IU/mg <sup>c</sup>	$\mu\text{g/mL}^b$	IU/mg <sup>c</sup>	$\mu\text{g/mL}^d$	IU/mg <sup>c</sup>	$\mu\text{g/mL}^d$	IU/mg <sup>c</sup>	$\mu\text{g/mL}^d$	IU/mg <sup>c</sup>
FCS- <i>Ib</i> 18-mer	46.5	54.7	>128	<14.6	324	<1.00	7.61	13.1	0.43	180
FCS- <i>Ib</i> 15-mer	62.7	40.5	>128	<14.6	>1000	<1.00	12.6	7.90	0.52	148
FCS- <i>Ib</i> 12-mer	97.7	26.0	>256	<7.30	>1000	<1.00	24.5	4.08	0.80	96.8
FCS- <i>Ib</i> 9-mer	160	15.8	>256	<7.30	>1000	<1.00	271	<1.00	1.48	52.1
FCS- <i>Ib</i> 6-mer	>256	~7.00	>512	<3.65	>1000	<1.00	>1000	<1.00	16.5	4.66
FCS- <i>Pg</i> 18-mer	61.4	41.4	>128	<14.6	480	<1.00	9.28	10.8	0.61	125
FCS- <i>Pg</i> 15-mer	89.2	28.5	>128	<14.6	>1000	<1.00	17.0	5.87	0.90	85.4
FCS- <i>Pg</i> 12-mer	129	19.7	>256	<7.30	>1000	<1.00	35.8	2.79	1.43	54.0
FCS- <i>Pg</i> 9-mer	190	13.4	>256	<7.30	>1000	<1.00	374	<1.00	2.59	29.8
FCS- <i>Pg</i> 6-mer	>256	~7.00	>512	<3.65	>1000	<1.00	>1000	<1.00	21.2	3.64
UFH	12.0	212	8.81	212	0.50	212	0.47	212	0.36	212
LMWH	36.5	69.6	33.1	56.4	1.53	69.2	0.88	113	1.39	55.4

<sup>a</sup>The APTT and TT of FCS-*Ib* oligomers were cited from our previous publication.<sup>14</sup> <sup>b</sup>Concentration required to double the APTT/TT of human plasma (APTT/TT doubling). <sup>c</sup>The activity was expressed as international units per milligram (IU/mg) using a parallel standard curve based on the international heparin standard (212 IU/mg). <sup>d</sup>IC<sub>50</sub> value, the concentration required to inhibit 50% of protease activity.

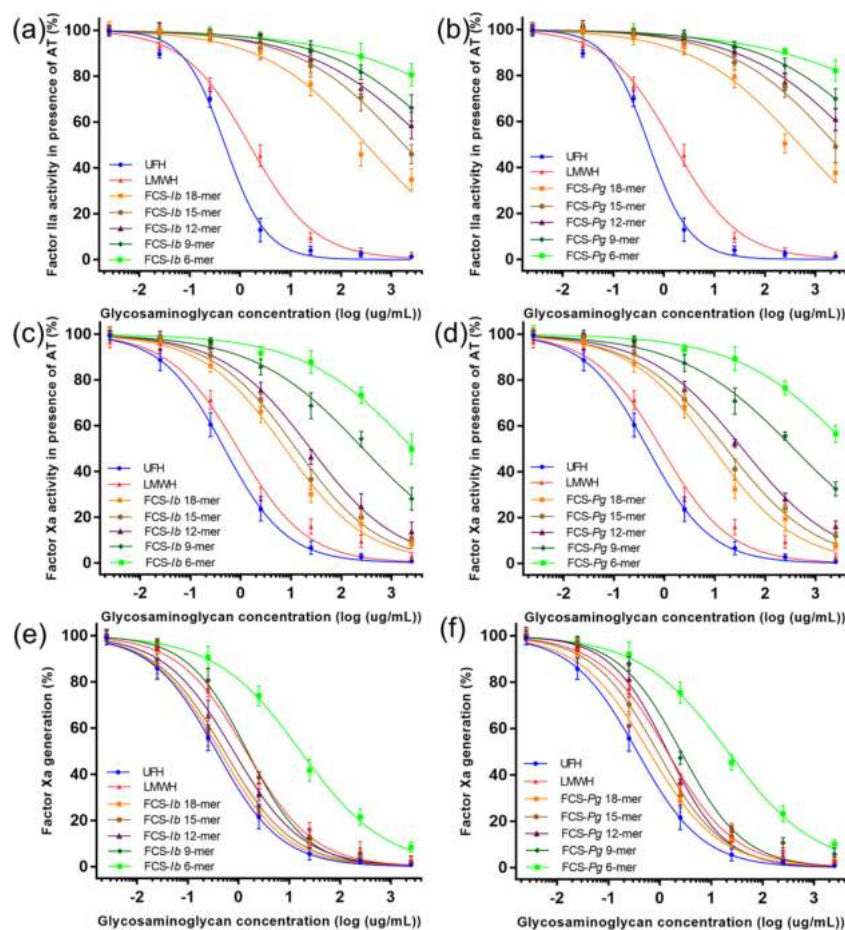


**Figure 3.** Effects of FCS-*Ib* oligomers on (a) FIIa and (c) FXa activities in the presence of antithrombin (AT) and (e) intrinsic FXase activity. Effects of FCS-*Pg* oligomers on (b) FIIa and (d) FXa activities in the presence of AT and (f) intrinsic FXase activity. The results are expressed as means  $\pm$  the standard deviation ( $n = 3$ ). See Table 1 for IC<sub>50</sub> values.

We next compared the effects of the FCS oligomers on coagulation factors with a cofactor, including anti-FIIa/AT, anti-FXa/AT, and anti-FXase to further investigate the

mechanism of their action on the intrinsic clotting pathway. The results are shown in Figure 3 and Table 1. All of the activities of these oligomers were concentration-dependent,



Table 2. Binding Affinities of the FCS Oligomer with a Coagulation Factor or Cofactor by Competitive Binding Experiment<sup>a</sup>

compd	FIIa (100 nM)			FXa (500 nM)			AT (500 nM)			FIXa (500 nM)		
	$\mu\text{M}^b$	$\mu\text{g/mL}^c$	$K_i$ (M) <sup>d</sup>	$\mu\text{M}^b$	$\mu\text{g/mL}^c$	$K_i$ (M) <sup>d</sup>	$\mu\text{M}^b$	$\mu\text{g/mL}^c$	$K_i$ (M) <sup>d</sup>	$\mu\text{M}^b$	$\mu\text{g/mL}^c$	$K_i$ (M) <sup>d</sup>
FCS- <i>Ib</i> 18-mer	3.65	18.4	$1.58 \times 10^{-6}$	4.95	24.9	$3.25 \times 10^{-7}$	1.8	9.1	$9.94 \times 10^{-7}$	0.9	4.5	$2.05 \times 10^{-7}$
FCS- <i>Ib</i> 15-mer	5.25	22.0	$2.27 \times 10^{-6}$	8.6	36.0	$5.64 \times 10^{-7}$	2.2	9.2	$1.21 \times 10^{-6}$	1.3	5.4	$2.96 \times 10^{-7}$
FCS- <i>Ib</i> 12-mer	7.7	25.7	$3.33 \times 10^{-6}$	10.2	34.1	$6.69 \times 10^{-7}$	3.95	13.2	$2.18 \times 10^{-6}$	2.4	8.0	$5.47 \times 10^{-7}$
FCS- <i>Ib</i> 9-mer	8.2	20.5	$3.55 \times 10^{-6}$	20.8	51.9	$1.36 \times 10^{-6}$	4.7	11.7	$2.59 \times 10^{-6}$	2.85	7.1	$6.50 \times 10^{-7}$
FCS- <i>Ib</i> 6-mer	16.8	27.7	$7.27 \times 10^{-6}$	57.5	94.9	$3.77 \times 10^{-6}$	13.8	22.8	$7.62 \times 10^{-6}$	7.65	12.6	$1.74 \times 10^{-6}$
FCS- <i>Pg</i> 18-mer	5.2	26.2	$1.78 \times 10^{-6}$	14	70.4	$9.02 \times 10^{-7}$	2.5	12.6	$5.65 \times 10^{-6}$	1.75	8.8	$2.88 \times 10^{-7}$
FCS- <i>Pg</i> 15-mer	7.2	30.1	$2.46 \times 10^{-6}$	20.8	87.1	$1.34 \times 10^{-6}$	6.3	26.4	$1.42 \times 10^{-5}$	2.4	10.0	$3.95 \times 10^{-7}$
FCS- <i>Pg</i> 12-mer	8.8	29.4	$3.01 \times 10^{-6}$	22	73.5	$1.42 \times 10^{-6}$	25	83.5	$5.65 \times 10^{-5}$	3.65	12.2	$6.00 \times 10^{-7}$
FCS- <i>Pg</i> 9-mer	12.5	31.2	$4.28 \times 10^{-6}$	39.5	98.6	$2.54 \times 10^{-6}$	$\gg 25$	$\gg 62.4$	$\gg 5.65 \times 10^{-5}$	4.95	12.4	$8.14 \times 10^{-7}$
FCS- <i>Pg</i> 6-mer	23.5	38.8	$8.04 \times 10^{-6}$	82.8	136.7	$5.33 \times 10^{-6}$	$\gg 50$	$\gg 82.6$	$\gg 1.13 \times 10^{-4}$	16	26.4	$2.63 \times 10^{-6}$

<sup>a</sup>The detailed SPR competition sensorgrams are shown in Figures S12–S15. <sup>b</sup> $\text{IC}_{50}$  value of the FCS oligomer molar concentration required to reach 50% of binding competition. <sup>c</sup> $\text{IC}_{50}$  value of the FCS oligomer mass concentration required to reach 50% of binding competition. <sup>d</sup> $K_i$  is the binding affinity of the FCS oligomer for the coagulation factor or cofactor, and it is calculated by the Cheng–Prusoff formula  $K_i = \text{IC}_{50}/(1 + C/K_D)$ ,<sup>36,37</sup> where  $C$  is the concentration of the coagulation factor or cofactor and  $K_D$  is the binding affinity of native FCS for the coagulation factor or cofactor.

and their strength decreased with a decrease in molecular size. The 9-mers to 18-mers prepared from both FCS-*Ib* and FCS-*Pg* showed potent inhibition of the intrinsic FXase, weak inhibition of FXa in the presence of AT, and almost no inhibition of FIIa in the presence of AT. Both the FCS-*Ib* 6-mer and the FCS-*Pg* 6-mer showed a very weak inhibition of the intrinsic FXase. For a given molecular size, the FCS-*Ib* oligomer showed stronger inhibition of the intrinsic FXase and inhibition of FXa in the presence of AT than the FCS-*Pg* oligomer. These results were consistent with the APTT assay data. Remarkably, the anti-FXase activity of these FCS oligomers was >10-fold higher than their anti-FXa/AT activity, and the difference between these two intensities increased with a decrease in molecular size. This result suggested that the anti-FXase activity of both FCS-*Ib* and FCS-*Pg* oligomers is responsible for their intrinsic anticoagulant activity. Furthermore, the intrinsic anticoagulant activity of FCS oligomers showed more dependence on their anti-FXase activity when their molecular size is closer to the 9-mer.

**FCS Oligomers Exhibit the Strongest Binding Affinity with FIXa among Coagulation Factors and AT.** We next investigated the interactions of these 10 FCS oligomers with FIIa, FXa, AT, and FIXa using surface plasmon resonance (SPR) to further understand their anticoagulant mechanism. First, we investigated the interactions of coagulation factors or AT with native FCS polysaccharides and unfractionated heparin (UFH) (Figure S11 and Table S3). Our results showed that both FCS-*Ib* and FCS-*Pg* polysaccharides could bind FIIa, FXa, and FIXa with affinities higher than those of UFH, but they bound to AT with affinities lower than those of UFH. The interactions between GAGs and proteins all fit well using a 1:1 (Langmuir) binding model. The binding affinities of FCS-*Ib* for FIIa ( $K_D = 4.33 \times 10^{-8}$  M) and FCS-*Pg* with FIIa ( $K_D = 3.42 \times 10^{-8}$  M) were similar and were ~10-fold stronger than the binding affinity of UFH with FIIa ( $K_D = 3.70 \times 10^{-7}$  M). The binding affinities of FCS-*Ib* with FXa ( $K_D =$

$3.28 \times 10^{-8}$  M), FCS-*Pg* with FXa ( $K_D = 3.22 \times 10^{-8}$  M), and UFH with FXa ( $K_D = 1.62 \times 10^{-8}$  M) were very similar. The binding affinities of FCS-*Ib* with FIXa ( $K_D = 1.14 \times 10^{-7}$  M), FCS-*Pg* with FIXa ( $K_D = 8.22 \times 10^{-8}$  M), and UFH with FIXa ( $K_D = 1.84 \times 10^{-7}$  M) were also very similar. However, the binding affinity of UFH for AT ( $K_D = 5.39 \times 10^{-8}$  M) was ~5-fold stronger than the binding affinity of FCS-*Ib* for AT ( $K_D = 2.76 \times 10^{-7}$  M) and ~20-fold stronger than the binding affinity of FCS-*Pg* for AT ( $K_D = 1.13 \times 10^{-6}$  M). All of these results were consistent with previous reports on binding affinities of a depolymerized FCS ( $M_w \sim 14$  kDa) with coagulation factors or cofactors measured by biolayer interferometry (BLI).<sup>32</sup> In addition, these results suggested that the anticoagulant activities of native FCSs and FCS oligosaccharides were mainly mediated through direct binding to various coagulation factors.

The binding affinity of the FCS oligomer with the coagulation factor or AT was next examined by competitive binding experiments. For example, FIIa (100 nM) was preincubated with gradient concentrations of FCS-*Ib* 18-mer prior to interacting with immobilized FCS-*Ib* to investigate the binding affinity of the FCS-*Ib* 18-mer with FIIa. If the FCS-*Ib* 18-mer interacted with FIIa, the amount of FIIa binding to immobilized FCS-*Ib* would be reduced, resulting in a weaker resonance unit (RU) signal. This method indirectly measures the binding affinity of the FCS-*Ib* 18-mer for FIIa and has been successfully used in studying the interactions between various proteins and polysaccharides.<sup>33–35</sup> As shown in Figure S12a, with an increase in the concentrations of the FCS-*Ib* 18-mer in solution, the level of binding between FIIa and immobilized FCS-*Ib* was gradually reduced. The maximal binding affinity of FIIa with immobilized FCS-*Ib* was ~1013 RU when there was no FCS-*Ib* 18-mer in the solution. The maximal binding affinity of FIIa for immobilized FCS-*Ib* was reduced to ~132 RU when there was 25  $\mu\text{M}$  FCS-*Ib* 18-mer in the solution, indicating that the free percentage of FIIa was only 13%.



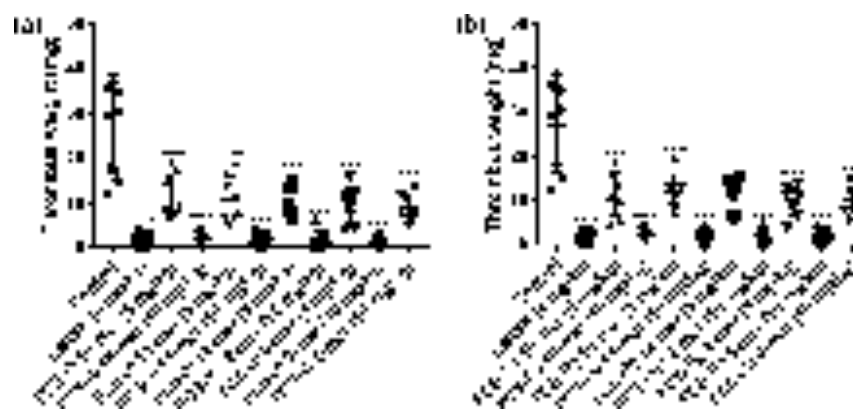


**Figure 4.** Venous antithrombotic activity of (a) FCS-*Ib* oligomers and (b) FCS-*Pg* oligomers *in vivo*. Antithrombotic activity was investigated in male Sprague-Dawley rats with the rabbit brain thromboplastin-induced venous thrombosis model. The results are expressed as thrombus weight (mean  $\pm$  the standard deviation;  $n = 8$ ; \*\*\* $P < 0.001$  vs control).

Competitive binding experiments confirmed the interaction between the FCS-*Ib* 18-mer and FIIa. Once the binding sites of FIIa were occupied by the FCS-*Ib* 18-mer, they could not be replaced with immobilized FCS-*Ib*, indicating that the FCS-*Ib* 18-mer shows fairly strong binding affinity with FIIa. According to competitive binding experiments with various concentrations of the FCS-*Ib* 18-mer, the  $IC_{50}$  value required to reach 50% of binding competition was obtained at  $\sim 3.85 \mu\text{M}$ . We then used the Cheng–Prusoff formula  $K_i = IC_{50}/(1 + C/K_D)^{36,37}$  to calculate the binding affinity of the FCS-*Ib* 18-mer for FIIa ( $K_i$ ) to be  $1.67 \times 10^{-6} \text{ M}$ , which is approximately 1/40th of FCS-*Ib*–FIIa binding affinity ( $K_D = 4.33 \times 10^{-8} \text{ M}$ ).

We determined the binding affinities of other FCS oligomers for coagulation factors or AT by using FCS oligomer concentrations required to reach 50% of binding competition (Table 2). In all competitive binding tests, the  $IC_{50}$  molar values for the FCS oligomers increased with a decrease in molecular size. The binding affinity of the FCS oligomer for the coagulation factor or AT also decreased with a decrease in molecular size. Both types of oligomers from the 9-mer to the 6-mer showed an even more pronounced decrease in binding affinity with a coagulation factor or AT. Among the coagulation factors and AT, FIXa showed higher binding affinities for FCS oligomers than FIIa and AT, explaining the selective anti-FXase activities of FCS 9–18 oligomers. For the same molecular size, the FCS-*Ib* oligomers showed some stronger binding affinity with coagulation factors and AT, indicating that FCS oligomers with 2,4-disulfated Fuc branches have stronger binding affinity for these proteins than those with 3,4-disulfated Fuc branches. When the  $IC_{50}$  molar values were turned into  $IC_{50}$  mass values, it indicated that all FCS-*Ib* 9–18 oligomers or all FCS-*Pg* 9–18 oligomers showed similar inhibitory effects on coagulation factors, especially on FIXa.

**FCS 9–18 Oligomers Exhibit Molecular Size-Independent Potent Antithrombotic Activity *In Vivo*.** We next investigated and compared the *in vivo* antithrombotic activity of both types of FCS 6-mer to 18-mer through a rabbit brain thromboplastin-induced venous thrombosis model.<sup>13</sup> FCS oligomers or the LMWH (enoxaparin, positive control) were administered dorsally and subcutaneously to male Sprague-Dawley rats before inducing the venous thrombosis. As shown in Figure 4, both types of FCS 9-mer to 18-mer exhibited similarly strong inhibition of venous thrombus

formation with an inhibition rate of 92–95% at a dose of 10 mg/kg. This effect was close to that of LMWHs at a dose of 4 mg/kg. Additionally, FCS 9–18 oligomers exhibited similarly strong inhibition of venous thrombus formation with an inhibition rate of 55–65% at a dose of 5 mg/kg. Although these FCS 9–18 oligomers showed anticoagulant activities and binding affinity for various clotting factors commensurate with their molecular size and the sulfation pattern on Fuc branches *in vitro*, all of these FCS oligomers showed similar antithrombotic activities *in vivo* at two doses. This indicated that inhibiting thrombogenesis is much more complex than inhibiting a single anticoagulant factor. From the result of  $IC_{50}$  mass values in Table 2, it showed that all FCS-*Ib* 9–18 oligomers at a concentration of 4.5–7.1  $\mu\text{g}/\text{mL}$  could inhibit half of 500 nM FIXa, and all FCS-*Pg* 9–18 oligomers at a concentration of 8.8–12.4  $\mu\text{g}/\text{mL}$  could inhibit half of 500 nM FIXa. Thus, the same concentration of FCS 9–18 oligomers has an inhibition ability similar to that of FIXa. Although both FCS-*Ib* 6-mer and FCS-*Pg* 6-mer exhibited much weaker anticoagulant activities, they could still interact with a variety of coagulation factors, which caused thrombosis inhibition rates of 66% and 62% at a dose of 10 mg/kg, respectively. Overall, the antithrombotic properties of these FCS oligomers can be attributed to their interaction with various clotting factors, particularly FIXa, finally inhibiting the generation of venous thrombosis.

**FCS Oligomers Are Rapidly Absorbed after Subcutaneous Administration.** We tracked the absorption and metabolism of two types of fluorescently labeled FCS oligomers mainly including 6–18 oligomers after subcutaneous administration to rats to determine how long FCS oligomers serve as anticoagulants and antithrombotic agents in the body. First, fluorescein isothiocyanate (FITC) was used to label the two types of FCS oligomers as shown in Figure S16. Ultraviolet (UV) scanning spectra indicated that these FITC-labeled FCS oligomers showed UV absorbance at  $\sim 490 \text{ nm}$  (Figure S17). HPGPC profiles by refractive index detection indicate that FITC-labeled FCS oligomers show almost the same molecular size distributions as the original FCS oligomers (Figure S18a,b). HPGPC profiles of FITC-labeled FCS oligomers by the UV detector at 490 nm were similar to those obtained by refractive index detection, indicating that FITC labeling was uniform for different oligomers (Figure

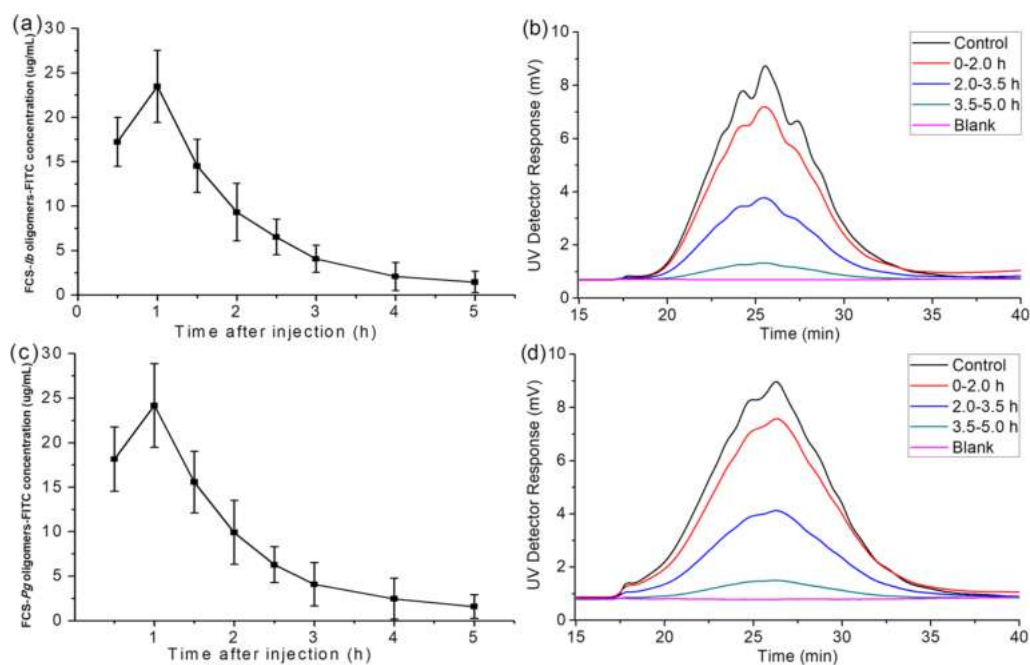


**Figure 5.** Absorption and metabolism of FCS oligomers after subcutaneous administration in rats. Concentration monitoring of (a) FCS-*Ib* FITC-labeled oligomers and (c) FCS-*Pg* FITC-labeled oligomers in blood. The half-lives ( $t_{1/2}$ ) of FCS-*Ib* FITC-labeled and FCS-*Pg* FITC-labeled oligomers in the blood 1–5 h after administration were 1.00 and 1.02 h, respectively. HPGPC profiles of the urine samples at different periods after subcutaneous administration of (b) FCS-*Ib* FITC-labeled oligomers and (d) FCS-*Pg* FITC-labeled oligomers. The control was FITC-labeled FCS oligomers (1 mg/mL), and the blank was the urine before injection. Samples were analyzed using a Superdex Peptide 10/300 GL column (10 mm  $\times$  300 mm) by a UV detector at 490 nm while using 0.2 M NaCl as the eluent at a flow rate of 0.4 mL/min.

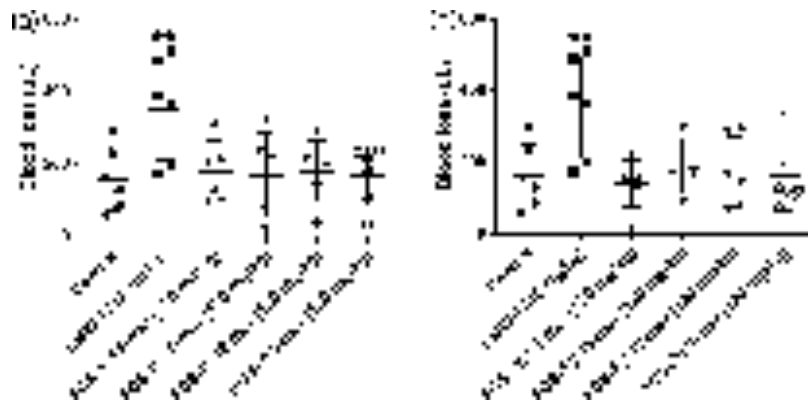


**Figure 6.** Bleeding effect of (a) FCS-*Ib* oligomers and (b) FCS-*Pg* oligomers *in vivo*. The LMWH (enoxaparin, positive control) or FCS oligomers were administered dorsally and subcutaneously to male Kunming mice. Blood loss was determined by measuring the hemoglobin present in the water using a spectrophotometric method. The results are expressed as microliters of blood loss (mean  $\pm$  the standard deviation;  $n = 6$ ;  $**P < 0.01$  vs control).

S18c,d). Fluorescence scanning spectra of the two types of FITC-labeled FCS oligomers both show maximum excitation wavelengths (Ex) at  $\sim 450$  nm and maximum emission wavelengths (Em) at  $\sim 510$  nm, similar to those of FITC (Figure S19).

After successful FITC labeling, the two types of FITC-labeled FCS oligomers were subcutaneously administered to rats to determine their absorption and metabolism. Both FCS-*Ib* FITC-labeled and FCS-*Pg* FITC-labeled oligomers showed similar absorption–metabolism curves in the blood (Figure

Sa,c). FITC-labeled FCS oligomers rapidly appear in the blood at 0.5 h after subcutaneous administration. After  $\sim 1$  h, the concentration of FITC-labeled FCS oligomers in the blood reached its maximum before gradually decreasing. Within the next hour, the concentration of FITC-labeled FCS oligomers in blood is reduced to half of its peak value. Five hours after injection, the concentration of FITC-labeled FCS oligomers in blood was almost undetectable. From the absorption–metabolism curves 1–5 h after administration, we could calculate that the half-lives ( $t_{1/2}$ ) of FCS-*Ib* FITC-labeled and

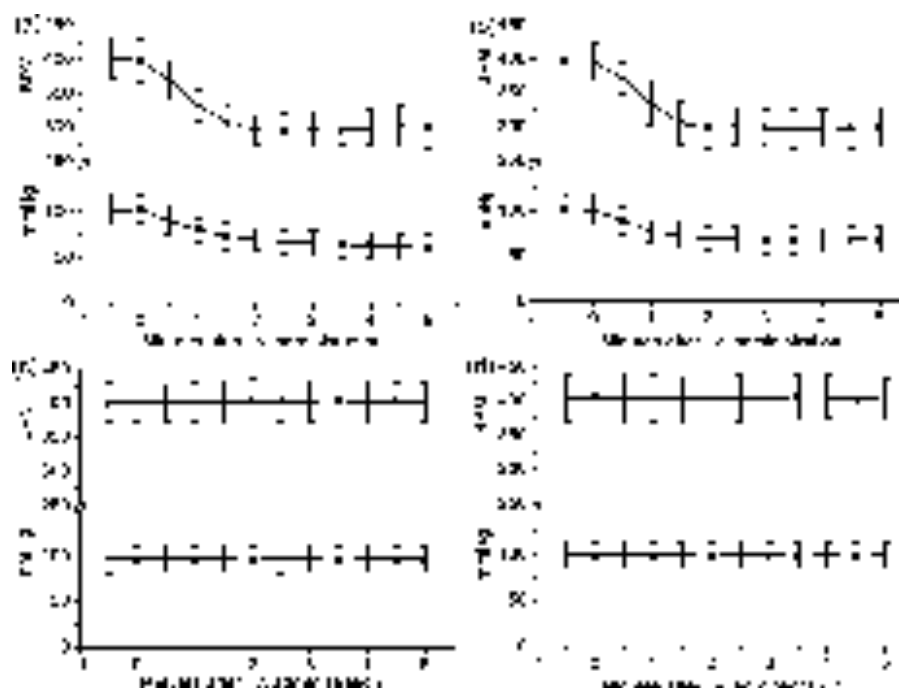


**Figure 7.** Effects of (a) FCS-Ib, (b) FCS-Pg, (c) the FCS-Ib 18-mer, and (d) the FCS-Pg 18-mer administered by intravenous injection on heart rate (●, BPM) and mean arterial blood pressure (■, mmHg) of male Sprague-Dawley rats. After a 10 min adaptation period, the rats were intravenously administered at 10 mg/kg of native FCS or FCS 18-mer as an aqueous solution, and then the systolic, diastolic blood pressures and the heart rate were continuously monitored. The results are expressed as means  $\pm$  the standard deviation ( $n = 5$ ).

**Table 3.** Relation between Molecular Information and the Influence on Platelet Aggregation of Different FCS-Ib Compounds

compd	$M_w$ ( $\times 10^3$ g/mol)	polydispersity ( $M_w/M_n$ )	Mark–Houwink–Sakurada $\alpha$	intrinsic viscosity $\eta$ (mL/g)	maximum aggregation (%) <sup>a</sup>
native FCS-Ib	70.09 $\pm$ 0.862	1.442 $\pm$ 0.046	0.538	78.54 $\pm$ 0.911	41.6
FCS-Ib D1	13.09 $\pm$ 0.256	1.609 $\pm$ 0.118	0.970	28.04 $\pm$ 0.175	23.1
FCS-Ib D2	9.994 $\pm$ 0.192	1.518 $\pm$ 0.091	0.605	14.89 $\pm$ 0.084	19.8
FCS-Ib D3	8.828 $\pm$ 0.428	1.556 $\pm$ 0.182	0.530	11.58 $\pm$ 0.015	15.0
FCS-Ib D4	7.350 $\pm$ 0.122	1.630 $\pm$ 0.077	0.493	10.32 $\pm$ 0.015	6.49
FCS-Ib D5	6.668 $\pm$ 0.120	1.671 $\pm$ 0.057	0.465	9.420 $\pm$ 0.091	6.13
FCS-Ib D6	6.022 $\pm$ 0.502	1.723 $\pm$ 0.232	0.432	8.714 $\pm$ 0.019	5.21
FCS-Ib D7 (18-mer)	5.398 $\pm$ 0.136	1.795 $\pm$ 0.097	0.443	7.850 $\pm$ 0.021	3.06
FCS-Ib D8 (15-mer)	4.550 $\pm$ 0.165	1.641 $\pm$ 0.087	0.465	6.912 $\pm$ 0.049	5.50
FCS-Ib D9 (12-mer)	3.546 $\pm$ 0.128	1.753 $\pm$ 0.109	0.439	6.269 $\pm$ 0.024	4.19

<sup>a</sup>The maximum aggregation values of platelets caused by different FCS-Ib compounds are cited from our previous publication.<sup>14</sup>

FCS-Pg FITC-labeled oligomers in the blood were 1.00 and 1.02 h, respectively. These results are consistent with previous reports that a depolymerized FCS ( $M_w \sim 12$  kDa) was nearly cleared in 6 h after intravenous administration in rats.<sup>38</sup> In these experiments, we collected urine samples at different times. The HPGPC profiles of these samples using UV detection at 490 nm are shown in panels b and d of Figure 5. The FITC-labeled FCS oligomers in urine show nearly the same molecular size distribution as the administered FITC-labeled FCS oligomers, indicating their reliable stability in the circulatory system. Moreover, the concentration changes of FITC-labeled FCS oligomers in urine reflected the levels observed in the blood. We could conclude that the appreciable quantity of both types of FCS 6-mer to 18-mer in the blood could be excreted through the kidneys without a degradative metabolism.

**FCS Oligomers Exhibit No Bleeding Risk *In Vivo*.** Our previous studies showed that subcutaneous administration of a mixture of the FCS-Pg 6-mer to 18-mer did not cause bleeding *in vivo*.<sup>25</sup> Both types of 9-mer to 18-mer were investigated independently for their bleeding risk to provide a more accurate assessment on this side effect. The LMWH (enoxaparin, positive control) or FCS oligomers were administered dorsally and subcutaneously into male Kunming mice before cutting 5 mm from the tip of the tail. Blood loss was determined by measuring the hemoglobin present in the water using a spectrophotometric method.<sup>13</sup> The results are expressed as microliters of blood loss as shown in Figure 6. Compared with the blood loss of the control group, both types of the FCS 9-mer to 18-mer did not result in obvious blood loss at doses of 120 mg/kg ( $P > 0.05$ ). In contrast, the LMWH caused obvious blood loss at doses of 40 mg/kg ( $P < 0.01$ ). These results suggest that these oligomers effectively result in

anticoagulant and antithrombotic effects and may be safer than LMWHs for clinical application in preventing bleeding.

**FCS Oligomers Exhibit No Hypotension or Platelet Aggregation Risk *In Vivo*.** Molecular size determines whether an FCS oligomer can activate human FXII leading to dangerous hypotension and a reduced heart rate.<sup>14,25</sup> We investigated the *in vivo* hypotension risk of both types of the FCS 18-mer and compared these to native FCS (Figure 7). Intravenous tail administration of FCS-*Ib* or FCS-*Pg* polysaccharides to rats immediately caused hypotension and a reduced heart rate, which were mostly caused by activating FXII.<sup>10</sup> After a continuous decrease for ~2 min, the blood pressure and heart rate level out at a value well below normal. In contrast, the administration of the FCS-*Ib* 18-mer or FCS-*Pg* 18-mer showed no obvious effect on blood pressure or heart rate in rats. This result was also mostly caused by the inactivation on FXII by the FCS-*Ib* 18-mer or FCS-*Pg* 18-mer with a sufficiently small molecular size.<sup>12</sup> We hypothesize that the smaller molecular size of the FCS 9-mer to 15-mer oligomers was insufficient to cause hypotension and a reduced heart rate.

The molecular size also determines whether an FCS oligomer can cause platelet aggregation.<sup>12–14</sup> Solutions of a series of FCS-*Ib* compounds were studied to determine their association with platelet aggregation (Table 3). FCS-*Ib* compounds of different molecular sizes exhibited entirely different chain conformations and intrinsic viscosities. The chain conformation characteristic constant, Mark–Houwink–Sakurada  $\alpha$  values of 0–0.5, reflects a rigid sphere in an ideal solvent. Values of 0.5–0.8 correspond to a random coil in a good solvent, and values of 0.8–2.0 correspond to a rigid or rodlike configuration (stiff chain).<sup>39</sup> The native FCS-*Ib* polysaccharide showed a random coil with a high intrinsic viscosity of 78.5 mL/g in solution and easily caused platelet aggregation (maximum aggregation of 42%). After depolymerization, some larger  $M_w$  compounds (FCS-*Ib* D1–D3) still showed a random coil or a stiff chain in solution, but their intrinsic viscosities were significantly decreased along with their decreased  $M_w$ . FCS-*Ib* D1–D3 caused a much lower aggregation maximum for platelets. Even lower- $M_w$  compounds (FCS-*Ib* D4–D9) became rigid spheres in solution, and their intrinsic viscosity continued to decrease with a decreased  $M_w$ . FCS-*Ib* D4–D9 did not result in platelet aggregation. On the basis of these results, we could conclude that the platelet aggregation caused by large FCS compounds is highly related with their chain conformation and intrinsic viscosity in solution. Both types of FCS 9-mer to 18-mer are sufficiently small with a rigid sphere conformation and a low intrinsic viscosity in solution to avoid platelet aggregation.

## SUMMARY AND CONCLUSIONS

In this study, we prepared and purified the FCS 6-mer to 18-mer from two types of sea cucumbers, *Ib* and *Pg*. FCS oligomer structural analysis, performed by NMR and ESI-FTMS spectroscopy, confirmed that they were all comprised of trisaccharide repeating units of the structure L-Fuc2/3,4diS- $\alpha$ 1,3-D-GlcA- $\beta$ 1,3-{D-GalNAc4,6diS- $\beta$ 1,4-[L-Fuc2/3,4diS- $\alpha$ 1,3-D-GlcA- $\beta$ 1,3-] $_n$ -D-an-Tal-ol4,6diS ( $n = 1–5$ ), and the only distinction of the oligomers prepared from different sea cucumbers was their Fuc branch sulfation pattern. We next compared their anticoagulant activities *in vitro*, including APTT, TT, anti-FIIa/AT, anti-FXa/AT, and anti-FXase. The 9-mer to 18-mer of both types of FCS oligomers mainly

showed effects on the intrinsic clotting pathway through inhibition of the FXase. SPR competitive experiments verified that these FCS oligomers exhibit the greatest binding affinity for FIXa among various clotting proteins. Both the blood coagulation assays and SPR measurements indicated that the anticoagulant activities of these FCS oligomers vary with the molecular size and Fuc branch sulfation pattern. However, all sizes of FCS 9–18 oligomers with 2,4-disulfated or 3,4-disulfated Fuc branches exhibited similar *in vivo* antithrombotic effects. Both types of FCS 6-mers also showed favorable antithrombotic activity *in vivo*, although they showed weak anticoagulant *in vitro*.

In conclusion, we proposed the mechanism for the use of FCS oligomers for inhibiting thrombosis in blood vessels. On the basis of the blood coagulation assays and SPR measurements, FCS oligomers in the blood can interact with multiple clotting proteins, including FIXa, FXa, and FIIa to inhibit the coagulation pathway.<sup>40</sup> The most significant is the interaction with FIXa to inhibit FXase, preventing the generation of FXa. Meanwhile, these FCS oligomers could also interact with FXa to prevent the generation of FIIa and interact weakly with FIIa to prevent the generation of fibrin. In addition, at the same mass dose of FCS oligomers, although the binding affinities of the smaller oligomers are relatively weak, their molar concentration is relatively higher, giving these more opportunity to interact with clotting factors once they enter the blood circulation. Thus, these FCS oligomers achieve a similar *in vivo* antithrombotic effect.

By FITC labeling, we found that both types of FCS 6-mer to 18-mer were rapidly absorbed into the blood after subcutaneous administration in rats and appreciable quantities of them were cleared through the kidneys in ~5 h. Evaluation of the side effect indicated that none of the FCS 9–18 oligomers caused bleeding or hypotension in rats. Furthermore, FCS 9–18 oligomers were sufficiently small to behave as rigid spheres with low intrinsic viscosity in solution, avoiding platelet aggregation. Thus, they should be suitable for the large-scale preparation for clinical evaluation in antithrombotic applications.

## METHODS

**Materials.** The native FCS-*Pg* polysaccharide was isolated and purified from the sea cucumber *Pg*, as previously described.<sup>41</sup> Controlled depolymerization of the FCS-*Pg* polysaccharide was accomplished through partial N-deacetylation–deaminative cleavage as previously described.<sup>14</sup> The depolymerized FCS-*Pg* polysaccharide was fractionated by gel filtration on a Superdex 30 prep grade column (2.6 cm  $\times$  120 cm, GE Healthcare Life Sciences) with 0.3 M  $\text{NH}_4\text{HCO}_3$  at a flow rate of 0.3 mL/min. The native FCS-*Ib* and different sizes of FCS-*Ib* oligomers were obtained in the same way as in our previous publication.<sup>14</sup> Finally, we obtained ~2 g of FCS oligomers mainly including 6–18 oligomers from 1 kg of each type of dry sea cucumber with optimized degradation. After separation of mixed oligomers by GPC, each size of highly purified oligomer was obtained in amounts of 50–100 mg. Unfractionated heparin (UFH) was obtained from Sigma (St. Louis, MO). The LMWH (enoxaparin, 0.4 mL  $\times$  4000 AXaIU) was obtained from Sanofi-Aventis. APTT assay kits, TT assay kits, a calcium chloride solution (0.02 M), and standard human plasma were obtained from Siemens Healthcare Diagnostics. Biophen Heparin Anti-FIIa kits, Biophen Heparin Anti-FXa kits, and a chromogenic assay kit for measuring FVIII: C in concentrates were obtained from Hyphen Biomed. Human coagulation FVIII was obtained from China Biologic Products, Inc. (Shandong, China). Human thrombin (FIIa), purified human factor Xa (FXa), human antithrombin (AT), and purified human factor IXa



(FIXa) were obtained from Hyphen Biomed. All other chemicals and reagents were of analytical grade.

**NMR Spectroscopy.** FCS oligomers were dissolved in 500  $\mu\text{L}$  of  $\text{D}_2\text{O}$  (99.9%), lyophilized three times to substitute the exchangeable protons, and then transferred to NMR microtubes after dissolving in 500  $\mu\text{L}$  of  $\text{D}_2\text{O}$ . NMR spectra were recorded on a Bruker (Madison, WI) model 600 spectrometer with topspin 3.2 software at 298.15 K.

**MS Spectroscopy.** ESI-LTQ-Orbitrap-FTMS (Thermo Fisher Scientific) was used to analyze FCS oligomers. Mobile phase A (MPA) consisted of 5 mM ammonium acetate prepared with HPLC grade water. Mobile phase B (MPB) consisted of 5 mM ammonium acetate prepared in 98% HPLC grade acetonitrile with 2% HPLC grade water. Then 50% MPA and 50% MPB eluent was used at a flow rate of 250  $\mu\text{L}/\text{min}$  run for 3 min after 3.0  $\mu\text{L}$  of purified FCS oligomers (5.0  $\mu\text{g}/\mu\text{L}$ ) had been injected. The source parameters for FTMS detection were optimized to minimize the in-source fragmentation and sulfate loss and maximize the signal-to-noise ratio in negative ion mode. The source parameters included a 4.2 kV spray voltage, a  $-40$  V capillary voltage, a  $-50$  V tube lens voltage, a 275  $^\circ\text{C}$  capillary temperature, a 30 L/min sheath flow rate, and a 6 L/min auxiliary gas flow. Better than 3 ppm of mass accuracy was obtained routinely by external calibration of mass spectra. All FT mass spectra were recorded at a resolution of 60000 with a mass range of 300–2000 Da.

**Measurement of Anticoagulant Activity.** The APTT and TT assays were determined with a coagulometer (RAC-120) using APTT and TT reagents and standard human plasma as previously described.<sup>8,10,14</sup> The results are expressed as international units per milligram using a parallel standard curve based on the international heparin standard (212 IU/mg). Antithrombin (anti-FIIa) and antifactor Xa (anti-FXa) activities in the presence of antithrombin (AT) and samples and inhibition of intrinsic factor Xase (factor IXa-factor VIIIa complex) in the presence of samples were carried out in a 96-well microtiter plate as previously described.<sup>12,14</sup> The absorbance change rate was proportional to the FIIa and FXa activity remaining in the incubation mixtures. The experimental results were expressed as the percent of control ( $n = 3$ ).  $\text{IC}_{50}$  values were obtained by fitting the data to a noncompetitive inhibition model for the samples according to Sheehan and Walke.<sup>42</sup>

**Studies of the Interaction between GAGs and Coagulation Factors or a Cofactor.** The interactions of GAGs (including FCS-Ib, FCS-Pg, and UFH) with coagulation factors or a cofactor (FIIa, FXa, AT, and FIXa) were measured using surface plasma resonance (SPR) on a BIAcore 3000 system while referring to similar publications.<sup>33–35</sup> Briefly, the biotinylated GAG was immobilized to an SA chip based on the manufacturer's protocol. Successful immobilization of GAG was confirmed by the observation of a  $>200$  resonance unit (RU) increase in the sensor chip. The commercial coagulation factor or cofactor was resuspended in HBS-EP buffer. Different dilutions of the coagulation factor or cofactor were injected at a flow rate of 30  $\mu\text{L}/\text{min}$ . At the end of the injection, the same buffer was passed over the sensor surface to facilitate dissociation. After dissociation, the sensor surface was regenerated by injecting 30  $\mu\text{L}$  of 2 M NaCl. The response was monitored as a function of time (sensorgram) at 25  $^\circ\text{C}$ .

**Competition of Coagulation Factors or Cofactor Binding to Immobilized Native FCSs by FCS Oligomers.** Competitive SPR experiments, using different sizes of FCS oligomers, were performed to compare the ability to bind to FIIa, FXa, FIXa, or AT.<sup>33–35</sup> A coagulation factor or cofactor was separately preincubated with gradient concentrations of the FCS oligomer and then injected over the native FCS chip at a flow rate of 30  $\mu\text{L}/\text{min}$ . After each injection and association, dissociation and regeneration were performed as described above.

**Inhibition of Venous Thrombosis.** Antithrombotic activity in rats was assessed using rabbit brain thromboplastin as the thrombogenic stimulus.<sup>13</sup> Male Sprague-Dawley rats (body weights of 250–300 g) were randomly segregated into 20 groups of eight animals each. The control group, the LMWH group, and FCS oligomer groups were administered dorsally and subcutaneously at a dose of 1 mL of 0.86% NaCl/kg of body weight, 4 mg of LMWH/kg

of body weight, and 5 or 10 mg of FCS oligomers/kg of body weight, respectively. After 60 min, rats were anesthetized with an intramuscular injection of 100 mg of ketamine/kg of body weight and 16 mg of xylazine/kg of body weight, the inferior vena cava and its branches were isolated, and the branch of inferior vena cava under the left renal vein was ligated. A volume of 1 mL of 2% tissue thromboplastin/kg of body weight was injected from the femoral vein. After 20 s, stasis was established by ligating the edge of the left renal vein. After a 20 min stasis, the cavity was then reopened, the ligated segment was opened longitudinally, and the thrombus formed was removed, rinsed, dried for 24 h at 50  $^\circ\text{C}$ , and then weighed. The results are reported as means with the standard deviation. All tests, including the following ones, followed the institutional guidelines for animal care and experimentation approved by the Animal Care Review Committee of Zhejiang University.

**Absorption and Metabolism of FCS Oligomers.** Male Sprague-Dawley rats (body weights of 250–300 g) were randomly segregated into two groups of five animals each to measure the absorption and metabolism of FCS oligomers. Two groups were administered dorsally and subcutaneously with 10 mg of FCS-Ib FITC-labeled oligomers and FCS-Pg FITC-labeled oligomers per kilogram of body weight, respectively. After 0.5, 1.0, 1.5, 2.0, 2.5, 3.0, 4.0, and 5.0 h, 0.3–0.5 mL of blood was collected from the tails and mixed with one-ninth of the volume of a sodium citrate solution (109 mM). After centrifugation at 3000g for 5 min, plasma was detected as FCS oligomers-FITC content with a fluorescence microplate (BioTek) from a standard curve based on Ex at 450 nm and Em at 510 nm. Meanwhile, each group's urine at periods of 0–2.0, 2–3.5, and 3.5–5.0 h was separately collected, combined, and filtered (0.22  $\mu\text{m}$  filter membrane, Millipore) for detecting FCS FITC-labeled oligomers by HPGPC with a UV detector at 490 nm.

**Bleeding Effects.** Blood loss was determined by measuring the hemoglobin present in the water using a spectrophotometric method.<sup>13</sup> Male Kunming mice (body weights of 18–22 g) were randomly segregated into 10 groups of six animals each. The control group, the LMWH group, and the FCS oligomer groups were administered dorsally and subcutaneously with 5 mL of 0.86% NaCl/kg of body weight, 40 mg of LMWH/kg of body weight, and 120 mg of FCS oligomers/kg of body weight, respectively. After 60 min, the tails of the mice were cut 5 mm from the tip and immersed in 40 mL of distilled water for 90 min at 37  $^\circ\text{C}$  while being stirred. The volume of blood was determined from a standard curve based on absorbance at 540 nm.

**Arterial Blood Pressure and Heart Rate.** Male Sprague-Dawley rats (body weights of 250–300 g) were randomly segregated into four groups of five animals each to measure the arterial pressure and heart rate. Rats were anesthetized with a combination of xylazine and ketamine as described previously, and a P10 catheter was inserted into both their right femoral vein and artery. The arterial catheter was connected to a pressure transducer (MP150, BIOPAC Systems Inc.) coupled to an acquisition system (AcqKnowledge, BIOPAC Systems Inc.). After a 10 min adaptation period, the rats were intravenously administered 10 mg of native FCS or FCS 18-mer/kg as an aqueous solution, and then the systolic and diastolic blood pressures and heart rate were continuously monitored. At the end of the observation period, the animals were euthanized using KCl (10 mg/kg).

**Molecular Information about FCS Compounds.** Molecular information about FCS compounds, including weight-average molecular weight ( $M_w$ ), polydispersity ( $M_w/M_n$ ), and chain conformation (Mark-Houwink-Sakurada  $\alpha$ ), in solution was recorded by size exclusion chromatography equipped with a multiangle laser light scattering system with a refractive index detector (SEC-MALLS-RI, Wyatt Technology). SEC columns (SB-806 HQ and SB-804 HQ, 7.8 mm  $\times$  300 mm, Shodex) were protected by a OHPak SB-G guard column (Shodex), and SEC was performed at 25  $^\circ\text{C}$ . The intrinsic viscosity ( $[\eta]$ ) was obtained using a viscometer (ViscoStar III, Wyatt Technology) and connected to the SEC-MALLS-RI system. The value of  $dn/dc$  (specific refractive index increment) was estimated to be 0.138 mL/g; 0.2 M NaCl containing 0.02%  $\text{NaN}_3$  (pH 7.0) was used as the mobile phase at a flow rate of

0.5 mL/min. The sample was dissolved directly in the mobile phase (2–5 mg/mL) and filtered through 0.22 mm filter membrane (Millipore). The injection volume was 50 mL and run for 100 min. Data acquisition and calculations were performed with ASTRA, version 7.1.2 (Wyatt Technology).

## ■ ASSOCIATED CONTENT

### Supporting Information

The Supporting Information is available free of charge at <https://pubs.acs.org/doi/10.1021/acscchembio.0c00439>.

Additional data about the FCS oligomers' NMR spectra with  $^1\text{H}$  and  $^{13}\text{C}$  chemical shifts, FCS oligomers' high-resolution FTMS spectrograms, SPR sensorgrams with a fitted curve and kinetic constants, SPR competition sensorgrams with  $\text{IC}_{50}$  curves, and preparation and characterization of FCS oligomers-FITC (PDF)

## ■ AUTHOR INFORMATION

### Corresponding Authors

**Robert J. Linhardt** – Center for Biotechnology & Interdisciplinary Studies and Department of Chemistry & Chemical Biology, Rensselaer Polytechnic Institute, Troy, New York 12180, United States; [orcid.org/0000-0003-2219-5833](https://orcid.org/0000-0003-2219-5833); Phone: +1-518-276-3404; Email: [linhar@rpi.edu](mailto:linhar@rpi.edu); Fax: +1-518-276-3405

**Shiguo Chen** – College of Biosystems Engineering and Food Science, National-Local Joint Engineering Laboratory of Intelligent Food Technology and Equipment, Zhejiang Key Laboratory for Agro-Food Processing, Integrated Research Base of Southern Fruit and Vegetable Preservation Technology, Zhejiang International Scientific and Technological Cooperation Base of Health Food Manufacturing and Quality Control, Zhejiang University, Hangzhou 310058, China; [orcid.org/0000-0002-6439-7735](https://orcid.org/0000-0002-6439-7735); Phone: +86-13116780577; Email: [chenshiguo210@163.com](mailto:chenshiguo210@163.com); Fax: +86-571-88982151

### Authors

**Lufeng Yan** – College of Biosystems Engineering and Food Science, National-Local Joint Engineering Laboratory of Intelligent Food Technology and Equipment, Zhejiang Key Laboratory for Agro-Food Processing, Integrated Research Base of Southern Fruit and Vegetable Preservation Technology, Zhejiang International Scientific and Technological Cooperation Base of Health Food Manufacturing and Quality Control, Zhejiang University, Hangzhou 310058, China; Center for Biotechnology & Interdisciplinary Studies and Department of Chemistry & Chemical Biology, Rensselaer Polytechnic Institute, Troy, New York 12180, United States

**Danli Wang** – College of Biosystems Engineering and Food Science, National-Local Joint Engineering Laboratory of Intelligent Food Technology and Equipment, Zhejiang Key Laboratory for Agro-Food Processing, Integrated Research Base of Southern Fruit and Vegetable Preservation Technology, Zhejiang International Scientific and Technological Cooperation Base of Health Food Manufacturing and Quality Control, Zhejiang University, Hangzhou 310058, China

**Yanlei Yu** – Center for Biotechnology & Interdisciplinary Studies and Department of Chemistry & Chemical Biology, Rensselaer Polytechnic Institute, Troy, New York 12180, United States

**Fuming Zhang** – Center for Biotechnology & Interdisciplinary Studies and Department of Chemistry & Chemical Biology, Rensselaer Polytechnic Institute, Troy, New York 12180, United States; [orcid.org/0000-0003-2803-3704](https://orcid.org/0000-0003-2803-3704)

**Xingqian Ye** – College of Biosystems Engineering and Food Science, National-Local Joint Engineering Laboratory of Intelligent Food Technology and Equipment, Zhejiang Key Laboratory for Agro-Food Processing, Integrated Research Base of Southern Fruit and Vegetable Preservation Technology, Zhejiang International Scientific and Technological Cooperation Base of Health Food Manufacturing and Quality Control, Zhejiang University, Hangzhou 310058, China

Complete contact information is available at: <https://pubs.acs.org/doi/10.1021/acscchembio.0c00439>

### Notes

The authors declare no competing financial interest.

## ■ ACKNOWLEDGMENTS

The authors are grateful to the National Key R&D Program of China (2018YFD0901101), the National Natural Science Foundation of China (31871815), and the 2018 Zhejiang University Academic Award for Outstanding Doctoral Candidates. The authors thank the China Scholarship Council for supporting Lufeng Yan studying at Rensselaer Polytechnic Institute for two years.

## ■ REFERENCES

- (1) Liu, J., and Linhardt, R. J. (2014) Chemoenzymatic synthesis of heparan sulfate and heparin. *Nat. Prod. Rep.* 31, 1676–1685.
- (2) Lee, A. Y. Y., Levine, M. N., Baker, R. I., Bowden, C., Kakkar, A. K., Prins, M., Rickles, F. R., Julian, J. A., Haley, S., Kovacs, M. J., and Gent, M. (2003) Low-molecular-weight heparin versus a coumarin for the prevention of recurrent venous thromboembolism in patients with cancer. *N. Engl. J. Med.* 349, 146–153.
- (3) Woodruff, S., Lee, A. Y. Y., Carrier, M., Feugere, G., Abreu, P., and Heissler, J. (2019) Low-molecular-weight-heparin versus a coumarin for the prevention of recurrent venous thromboembolism in high- and low-risk patients with active cancer: a post hoc analysis of the CLOT Study. *J. Thromb. Thrombolysis* 47, 495–504.
- (4) O'Donnell, M., and Weitz, J. I. (2003) Thromboprophylaxis in surgical patients. *Can. J. Surg.* 46, 129–135.
- (5) Van Rein, N., Biedermann, J. S., Van der Meer, F. J. M., Cannegieter, S. C., Wiersma, N., Vermaas, H. W., Reitsma, P. H., Kruip, M. J. H. A., and Lijfering, W. M. (2017) Major bleeding risks of different low-molecular-weight heparin agents: a cohort study in 12 934 patients treated for acute venous thrombosis. *J. Thromb. Haemostasis* 15, 1386–1391.
- (6) Crowther, M., and Lim, W. (2007) Low molecular weight heparin and bleeding in patients with chronic renal failure. *Curr. Opin. Pulm. Med.* 13, 409–413.
- (7) Mousa, S. A., Zhang, H., Aljada, A., Zhang, F., Arbit, E., Bender, L., Goldberg, M., and Linhardt, R. (2007) Pharmacokinetics and pharmacodynamics of oral heparin solid dosage form in healthy human subjects. *Blood* 110, 4009.
- (8) Chen, S., Xue, C., Yin, L. A., Tang, Q., Yu, G., and Chai, W. (2011) Comparison of structures and anticoagulant activities of fucosylated chondroitin sulfates from different sea cucumbers. *Carbohydr. Polym.* 83, 688–696.
- (9) Chen, S., Hu, Y., Ye, X., Li, G., Yu, G., Xue, C., and Chai, W. (2012) Sequence determination and anticoagulant and antithrombotic activities of a novel sulfated fucan isolated from the sea cucumber *Isostichopus badiionotus*. *Biochim. Biophys. Acta, Gen. Subj.* 1820, 989–1000.
- (10) Chen, S., Li, G., Wu, N., Guo, X., Liao, N., Ye, X., Liu, D., Xue, C., and Chai, W. (2013) Sulfation pattern of the fucose branch is important for the anticoagulant and antithrombotic activities of fucosylated chondroitin sulfates. *Biochim. Biophys. Acta, Gen. Subj.* 1830, 3054–3066.

- (11) Fonseca, R. J. C., Sucupira, I. D., Oliveira, S. N. M. C. G., Santos, G. R. C., and Mourao, P. A. S. (2017) Improved anticoagulant effect of fucosylated chondroitin sulfate orally administered as gastro-resistant tablets. *Thromb. Haemostasis* 117, 662–670.
- (12) Wu, M., Wen, D., Gao, N., Xiao, C., Yang, L., Xu, L., Lian, W., Peng, W., Jiang, J., and Zhao, J. (2015) Anticoagulant and antithrombotic evaluation of native fucosylated chondroitin sulfates and their derivatives as selective inhibitors of intrinsic factor Xase. *Eur. J. Med. Chem.* 92, 257–269.
- (13) Zhao, L., Wu, M., Xiao, C., Yang, L., Zhou, L., Gao, N., Li, Z., Chen, J., Chen, J., Liu, J., Qin, H., and Zhao, J. (2015) Discovery of an intrinsic tenase complex inhibitor: Pure nonasaccharide from fucosylated glycosaminoglycan. *Proc. Natl. Acad. Sci. U. S. A.* 112, 8284–8289.
- (14) Yan, L. F., Li, J. H., Wang, D. L., Ding, T., Hu, Y. Q., Ye, X. Q., Linhardt, R. J., and Chen, S. G. (2017) Molecular size is important for the safety and selective inhibition of intrinsic factor Xase for fucosylated chondroitin sulfate. *Carbohydr. Polym.* 178, 180–189.
- (15) Yin, R. H., Zhou, L. T., Gao, N., Li, Z., Zhao, L. Y., Shang, F. N., Wu, M. Y., and Zhao, J. H. (2018) Oligosaccharides from depolymerized fucosylated glycosaminoglycan: Structures and minimum size for intrinsic factor Xase complex inhibition. *J. Biol. Chem.* 293, 14089–14099.
- (16) Liu, H., Zhang, X., Wu, M., and Li, Z. (2018) Synthesis and anticoagulation studies of “short-armed” fucosylated chondroitin sulfate glycoclusters. *Carbohydr. Res.* 467, 45–51.
- (17) Zhang, X., Liu, H. Y., Lin, L. S., Yao, W., Zhao, J. H., Wu, M. Y., and Li, Z. J. (2018) Synthesis of fucosylated chondroitin sulfate nonasaccharide as a novel anticoagulant targeting intrinsic factor Xase complex. *Angew. Chem., Int. Ed.* 57, 12880–12885.
- (18) Zhang, X., Yao, W., Xu, X., Sun, H., Zhao, J., Meng, X., Wu, M., and Li, Z. (2018) Synthesis of fucosylated chondroitin sulfate glycoclusters: A robust route to new anticoagulant Agents. *Chem. - Eur. J.* 24, 1694–1700.
- (19) Myron, P., Siddiquee, S., and Al Azad, S. (2014) Fucosylated chondroitin sulfate diversity in sea cucumbers: a review. *Carbohydr. Polym.* 112, 173–178.
- (20) Soares, P. A. G., Ribeiro, K. A., Valente, A. P., Capille, N. V., Oliveira, S., Tovar, A. M. F., Pereira, M. S., Vilanova, E., and Mourao, P. A. S. (2018) A unique fucosylated chondroitin sulfate type II with strikingly homogeneous and neatly distributed alpha-fucose branches. *Glycobiology* 28, 565–579.
- (21) Gao, R. C., Wu, N., Li, Y., and Chen, S. G. (2014) Structures and anticoagulant activities of the partially mild acidic hydrolysis products of the fucosylated chondroitin sulfate from sea cucumber *Pearsonothuria graeffei*. *J. Carbohydr. Chem.* 33, 471–488.
- (22) Wu, M. Y., Xu, S. M., Zhao, J. H., Kang, H., and Ding, H. (2010) Physicochemical characteristics and anticoagulant activities of low molecular weight fractions by free-radical depolymerization of a fucosylated chondroitin sulphate from sea cucumber *Thelenata ananas*. *Food Chem.* 122, 716–723.
- (23) Wu, N., Ye, X. Q., Guo, X., Liao, N. B., Yin, X. Z., Hu, Y. Q., Sun, Y. J., Liu, D. H., and Chen, S. G. (2013) Depolymerization of fucosylated chondroitin sulfate from sea cucumber, *Pearsonothuria graeffei*, via Co-60 irradiation. *Carbohydr. Polym.* 93, 604–614.
- (24) Yang, J., Mou, J., Ding, D., and Wang, X. (2017) In vivo and in vitro antithrombus activities of depolymerized holothurian polysaccharides. *Int. J. Biol. Macromol.* 94, 364–369.
- (25) Yan, L., Wang, D., Zhu, M., Yu, Y., Zhang, F., Ye, X., Linhardt, R. J., and Chen, S. (2019) Highly purified fucosylated chondroitin sulfate oligomers with selective intrinsic factor Xase complex inhibition. *Carbohydr. Polym.* 222, 115025.
- (26) Shaklee, P. N., and Conrad, H. E. (1984) Hydrazinolysis of heparin and other glycosaminoglycans. *Biochem. J.* 217, 187–197.
- (27) Shively, J. E., and Conrad, H. E. (1976) Formation of anhydrosugars in the chemical depolymerization of heparin. *Biochemistry* 15, 3932–3942.
- (28) Mourao, P. A. S., Pereira, M. S., Pavao, M. S. G., Mulloy, B., Tollefsen, D. M., Mowinckel, M. C., and Abildgaard, U. (1996) Structure and anticoagulant activity of a fucosylated chondroitin sulfate from echinoderm - Sulfated fucose branches on the polysaccharide account for its high anticoagulant action. *J. Biol. Chem.* 271, 23973–23984.
- (29) Yan, L., Li, L., Li, J., Yu, Y., Liu, X., Ye, X., Linhardt, R. J., and Chen, S. (2019) Bottom-up analysis using liquid chromatography–Fourier transform mass spectrometry to characterize fucosylated chondroitin sulfates from sea cucumbers. *Glycobiology* 29, 755–764.
- (30) Zhao, L. Y., Lai, S. S., Huang, R., Wu, M. Y., Gao, N., Xu, L., Qin, H. B., Peng, W. L., and Zhao, J. H. (2013) Structure and anticoagulant activity of fucosylated glycosaminoglycan degraded by deaminative cleavage. *Carbohydr. Polym.* 98, 1514–1523.
- (31) Agyekum, I., Pepi, L., Yu, Y., Li, J., Yan, L., Linhardt, R. J., Chen, S., and Amster, I. J. (2018) Structural elucidation of fucosylated chondroitin sulfates from sea cucumber using FTICR-MS/MS. *Eur. J. Mass Spectrom.* 24, 157–167.
- (32) Xiao, C., Lian, W., Zhou, L. T., Gao, N., Xu, L., Chen, J., Wu, M. Y., Peng, W. L., and Zhao, J. H. (2016) Interactions between depolymerized fucosylated glycosaminoglycan and coagulation proteases or inhibitors. *Thromb. Res.* 146, 59–68.
- (33) Zhang, F., Zhang, Z., Lin, X., Beenken, A., Eliseenkova, A. V., Mohammadi, M., and Linhardt, R. J. (2009) Compositional analysis of heparin/heparan sulfate interacting with fibroblast growth factor-fibroblast growth factor receptor complexes. *Biochemistry* 48, 8379–8386.
- (34) Zhang, F., Aguilera, J., Beaudet, J. M., Xie, Q., Lerch, T. F., Davulcu, O., Colón, W., Chapman, M. S., and Linhardt, R. J. (2013) Characterization of interactions between heparin/glycosaminoglycan and adeno-associated virus. *Biochemistry* 52, 6275–6285.
- (35) Zhao, J., Liu, X., Kao, C., Zhang, E., Li, Q., Zhang, F., and Linhardt, R. J. (2016) Kinetic and structural studies of interactions between glycosaminoglycans and langerin. *Biochemistry* 55, 4552–4559.
- (36) Yung-Chi, C., and Prusoff, W. H. (1973) Relationship between the inhibition constant (KI) and the concentration of inhibitor which causes 50% inhibition (I50) of an enzymatic reaction. *Biochem. Pharmacol.* 22, 3099–3108.
- (37) Lazareno, S., and Birdsall, N. J. (1993) Estimation of competitive antagonist affinity from functional inhibition curves using the Gaddum, Schild and Cheng-Prusoff equations. *Br. J. Pharmacol.* 109, 1110–1119.
- (38) Imanari, T., Washio, Y., Huang, Y., Toyoda, H., Suzuki, A., and Toida, T. (1999) Oral absorption and clearance of partially depolymerized fucosyl chondroitin sulfate from sea cucumber. *Thromb. Res.* 93, 129–135.
- (39) Masuelli, M. A. (2014) Mark-houwink parameters for aqueous-soluble polymers and biopolymers at various temperatures. *J. Polym. Biopolym. Phys. Chem.* 2, 37–43.
- (40) Palta, S., Saroa, R., and Palta, A. (2014) Overview of the coagulation system. *Indian J. Anaesth.* 58, 515–523.
- (41) Li, J. H., Li, S., Zhi, Z. J., Yan, L. F., Ye, X. Q., Ding, T., Yan, L., Linhardt, R. J., and Chen, S. G. (2016) Depolymerization of fucosylated chondroitin sulfate with a modified fenton-system and anticoagulant activity of the resulting fragments. *Mar. Drugs* 14, 170.
- (42) Sheehan, J. P., and Walke, E. N. (2006) Depolymerized holothurian glycosaminoglycan and heparin inhibit the intrinsic tenase complex by a common antithrombin-independent mechanism. *Blood* 107, 3876–3882.